91. The X-Ray Crystal Structure and Packing of a Hexakis-adduct of C_{60}: Temperature Dependence of Weak C–H···O Interactions

by **Paul Seiler***, **Lyle Isaacs**, and **François Diederich**

Laboratorium für Organische Chemie, ETH-Zentrum, Universitätstrasse 16, CH–8092 Zürich

(21.II.96)

The crystal structure and packing of the C_{60} hexakis-adduct **1** has been determined from accurate X-ray diffraction measurements. The largest deformations on the C_{60} surface occur within the bridged pyracylene subunits; the bridgehead 6–6 bond lengths of the four cyclopropane and the two cyclohexene rings, attached in pseudo-octahedral positions, are close to 1.6 Å. Significant deformations also occur in the remaining part of the C_{60} skeleton, not bridged to any of the functional groups. The crystal packing, analyzed at 270, 230, and 180 K is characterized by a three-dimensional network of 14 weak C–H···O interactions. For most of these, H···O and C···O distances decrease on cooling the crystal specimen, indicating that they are attractive in nature. On the other hand, the shortest, nearly linear C(sp^3)–H···O contact seems to be repulsive, since cooling of the crystal specimen leads to significantly longer H···O and C···O distances and to a reduction of the C–H···O linearity. Probably as a result of this intermolecular expansion, strain is produced in the crystal. Depending on the crystal-mounting procedure, this can lead either to a disordered structure (below *ca.* 200 K), or to destruction of the crystal specimen.

1. Introduction. – Hexakis-adduct **1** has been synthesized recently *via* tether-directed functionalization of I_h-C_{60} [1]. The functional groups, consisting of the anchor-tether-cyclohexene moiety and three diethyl-malonate addends are attached in pseudo-octahedral positions on the C_{60} surface. According to ^{1}H-NMR investigations, the average symmetry of **1** in solution is C_{2v}, but in the crystal it is reduced to C_2, and, hence, there are

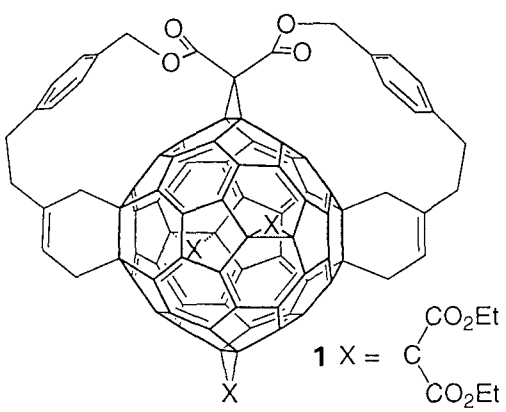

only four symmetry-independent addition sites. As a result of the different addends, the symmetry of the C_{60} skeleton itself is lowered from I_h to approximately D_{2h}. A brief description of the crystal structure has already appeared [2]. Analogous crystal structures of C_{60} hexakis-adducts have been published for a platinum derivative [3], and for a hexakis[di(ethoxycarbonyl)methano]-adduct [4].

In the present paper, we report additional structural details of **1** and some interesting aspects of the crystal packing, analyzed as a function of temperature.

2. Experimental. – 2.1. *General.* Bright-yellow single crystals of **1** were obtained by very slow evaporation of a benzene/MeCN soln. Since **1** is slightly air- and light-sensitive, it was stored under Ar in the dark. The X-ray measurements were performed on a *Nonius CAD4* diffractometer equipped with graphite monochromator (CuK_α radiation, $\lambda = 1.5418$ Å) and a *Nonius* gas-stream low-temperature device. The crystals belong to the monoclinic space group $C2/c$ with half a molecule of **1** and two half benzene molecules in the asymmetric unit. Hexakis-adduct **1** and benzene(1) lie on crystallographic twofold axes, benzene(2) lie on inversion centres.

2.2. *Structure Refinement.* The structure was solved by direct methods and refined by full-matrix least-squares analysis (SHELXTL PLUS), using an isotropic extinction correction and an exponentially modified weight factor $r = 5$ Å^2 [5]. Ordered heavy atoms were refined anisotropically, disordered atoms (see *Sect. 2.3*) isotropically and with half weights. H-Atoms were refined isotropically, using two different approaches. First, H-positions were based on configurational considerations and C–H distances of 0.96 Å (refinement A); then, H-atoms of CH, CH_2, and CH_3 groups involved in C–H···O interactions (see *Sect. 4*), were refined freely (refinement B). To examine whether the individual H-atoms were converging to the correct positions, two independent refinements were carried out, one with the calculated H-positions as input, the other with a starting set, with H-positions shifted by *ca.* 0.15 Å from these positions. Both refinements led to practically the same results, provided that the least-squares shifts were damped by a factor of *ca.* 0.7. Most of the refined C–H distances are in the range 0.9 to 1.1 Å; at 180 K, two C–H distances are close to 0.8 Å. The mean C–H distance obtained from the individual refinements is characteristically too short by *ca.* 0.12 Å. For the crystal-packing analysis, calculated and refined H-positions were moved along the corresponding C–H vector to give (idealized) C–H distances of 1.09 Å.

2.3. *Experimental Problems.* An initial data set (extending out to $H = 2\sin\theta/\lambda = 1.22$ Å^{-1}) was collected at 100 K, with a crystal specimen of linear dimensions of *ca.* 0.35 mm. This crystal was mounted on a glass fibre and embedded completely in epoxy resin to prevent evaporation of co-crystallized solvent. The crystal quality, judged by its scattering behavior, was satisfactory: low-order reflection profiles were quite symmetric and *ca.* 1.2° in width, reflection intensities could be observed to high *Bragg* angles, and the internal agreement factor based on 251 symmetry-equivalent reflection intensities was 0.018. The structure was solved in the centrosymmetric space group $C2/c$. However, least-squares refinements (heavy atoms anisotropic, H-atoms neglected) led to a surprisingly high $R(F)$ value of 0.22 and to a somewhat distorted molecular geometry. Additional refinements in the lower, non-centrosymmetric space group Cc gave a slightly better $R(F)$ value, but the molecular geometry was even worse, as a result of the expected high correlation among symmetry-related atoms. Because of this disappointing result, systematic absences were re-examined, and lattice parameters were measured as a function of temp. In the temp. range 270 to 100 K, neither a change of space group nor an abrupt change of the lattice parameters could be

Table 1. *Experimental Details of the X-Ray Analysis Used for the Determination of the Molecular Geometry of* **1**

Empirical formula	$½\ C_{110}H_{60}O_{16}\cdot C_6H_6$	No. of measured reflections	8637
Temp. of data collection [K]	230	No. of unique reflections	8342
Crystal dimensions [mm]	*ca.* 0.25 × 0.25 × 0.25	No. of observed reflections	
Space group	$C2/c$	($I > 2\sigma(I)$)	6061
Cell dimensions a [Å]	17.680(4)	No. of variables in final least-squares	
b [Å]	21.164(4)	analysis	663
c [Å]	21.740(4)	Type of refinement	F
β [°]	93.63(2)	Exponentially modified	
Formula weight	896.9	weight factor r [Å^2]	5.0
D_c [g/cm^3]	1.47	Extinction correction	isotropic
Max. $2\sin\theta/\lambda$ [Å^{-1}]	1.25	$R(F)$	0.049
Scan mode	ω/θ	$R_w(F)$	0.063

detected; in other words, there was no obvious indication of a phase transformation. On the other hand, *Fig. 1* shows that the thermal expansion coefficient $\alpha(a)$ below 180 K is practically zero. Since we were intrigued by the high $R(F)$ value and the atypical behavior of a, the structure was re-determined at four different temperatures, with two additional crystal specimens of linear dimensions of *ca.* 0.20 mm (crystal A) and 0.25 mm (crystal B), respectively. Crystal A was embedded again in epoxy resin and used for the measurements at 270, 180, and 100 K; crystal B was mounted with a trace of epoxy resin only and used for the measurement at 230 K. The four data sets obtained at 270, 230, 180, and 100 K have resolution limits of $H = 1.12$ Å^{-1}, 1.25 Å^{-1}, 1.18 Å^{-1}, and 1.18 Å^{-1}; the corresponding number of unique reflections and observed reflections with $I > 2\sigma(I)$ (given in parentheses) are 6071(4115), 8342(6061), 6843(5554), and 6625(5807), resp. The measuring procedure, given in *Table 1* for the most extensive data set, and the refinement procedure described above were always the same.

The main results of the four least-squares analyses can be summarized as follow. The diethyl-malonate bridge at C(55)–C(60) is disordered over two orientations at all temp., the population parameters of the disordered atoms being close to 0.5 (see *Figs. 2* and *3*). The remaining part of the structure is ordered at 270 and 230 K, ($R(F) = 0.049$), but 'disordered' at 180 and 100 K ($R(F) = 0.11$ and 0.15, resp.). This additional disorder expresses itself in artificially anisotropic displacement parameters and small residual electron-density peaks in the vicinity of various atoms, in particular at 100 K. Possibly it is a result of anharmonic thermal motion or of a second-order phase transition. Its nature has not been investigated any further. The much lower $R(F)$ value of 0.15 obtained at 100 K with the smaller crystal specimen shows that the degree of disorder differs significantly from one crystal specimen to another.

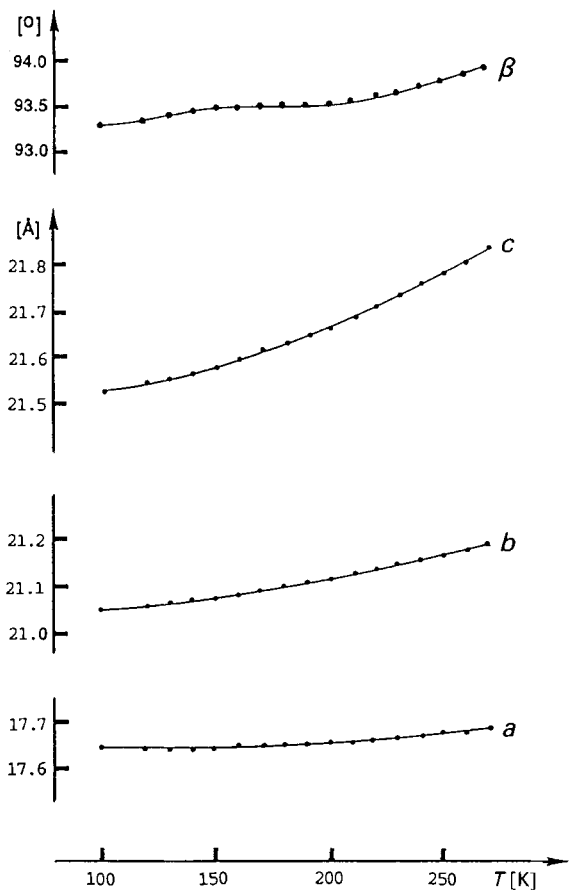

Fig. 1. *Temperature dependence of lattice parameters of* **1** *in the range 100–270 K*

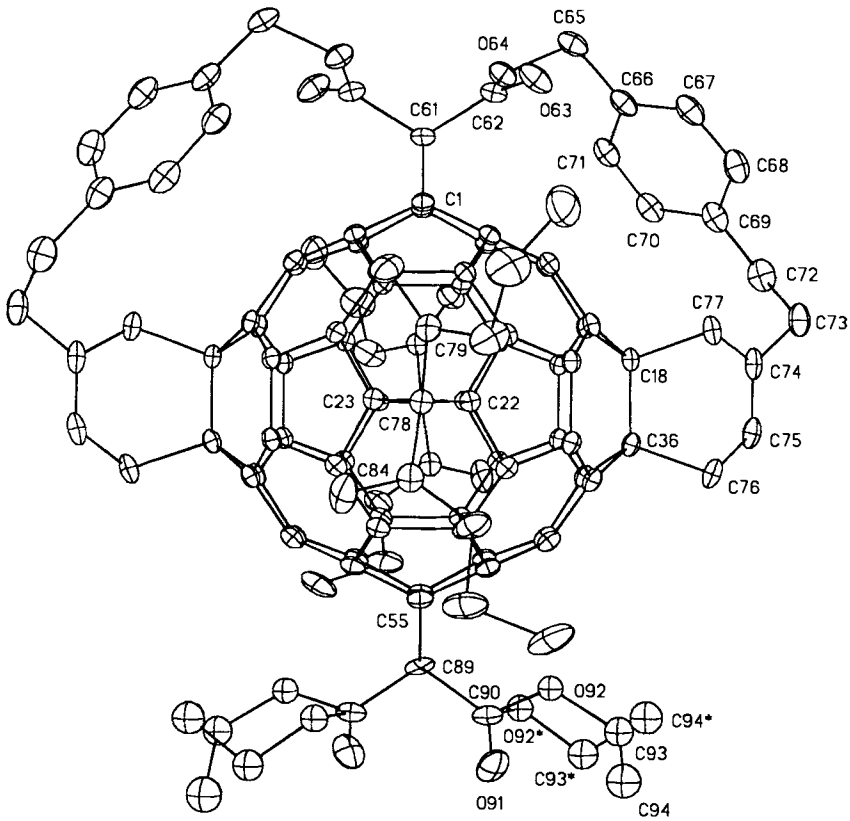

Fig. 2. *View of* **1**, *showing the atomic numbering of the anchor-tether-cyclohexene moiety and of the disordered diethyl-malonate addend.* Vibrational ellipsoids obtained at 230 K are drawn at the 30% probability level.

In the packing analysis of **1**, it is shown that C···O and H···O distances in contact (G) (extending roughly along *a*) increase on cooling the crystal specimen. This process must lead to increasing strain in the crystal specimen. In fact, additional experiments show that crystals not embedded in epoxy resin mostly shatter below *ca.* 200 K. So, to some extent the atypical contraction of *a* and the disorder obtained at low temp. must be attributed to our crystal-mounting procedure described for crystal A.

The molecular geometry discussed below is based on the measurement made with crystal B at 230 K. Exper. parameters of this analysis are summarized in *Table 1*, and further details are available on request from the *Cambridge Crystallographic Data Centre*, 12 Union Road, Cambridge CB12 1EZ (UK), on quoting the full journal citation.

3. Discussion of the Structure. – In a I_h-C_{60} fullerene (composed of 20 six-membered and 12 five-membered rings), there are 30 reactive 6–6 double bonds, which are accessible to addition reactions. The six addition sites in **1** are shown in *Figs. 2* and *3*. The molecule has C_2 symmetry; there are two pairs of symmetry-related bridgehead bonds, plus two (C(1)–C(2) and C(55)–C(60)) on a twofold axis. The numbering of the C_{60} skeleton used here follows that of *Taylor* [6]. Primed (′) and unprimed atoms are related by the twofold

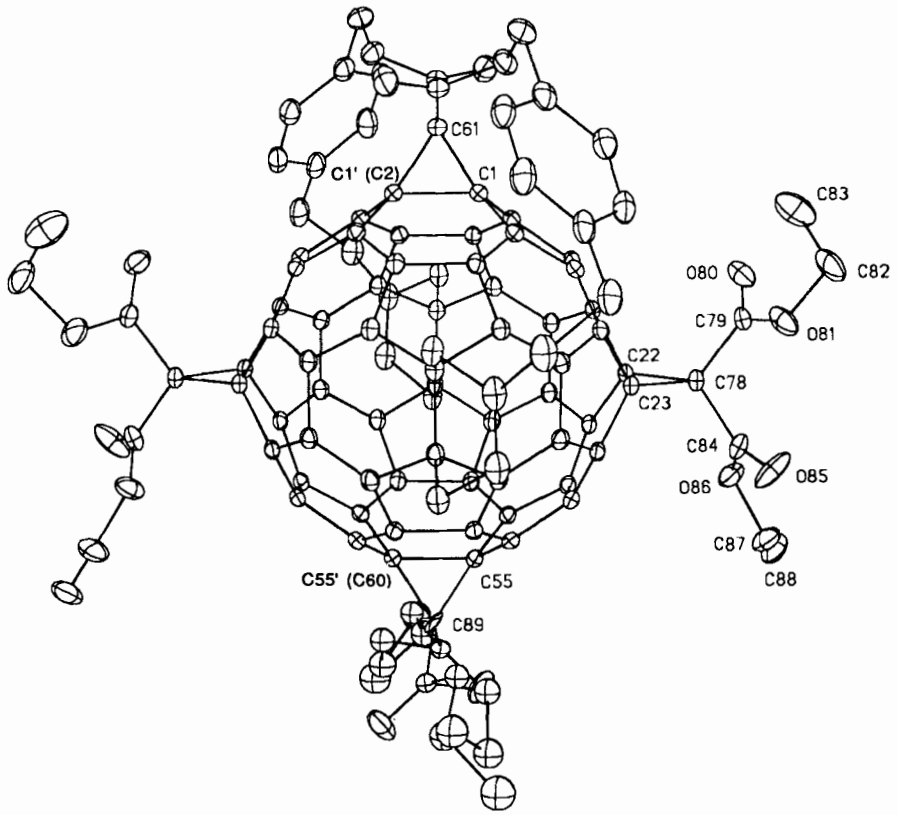

Fig. 3. *View of* **1**, *showing the atomic numbering of the ordered diethyl-malonate addends.* Vibrational ellipsoids obtained at 230 K are drawn at the 30% probability level.

axis (in *Fig. 3*, the corresponding numbering based on [6] is given in parentheses). Starred (*) and unstarred atoms within the diethyl-malonate bridge at C(55)–C(60) refer to the disorder described in *Experimental*. Estimated standard deviations (e.s.d.'s) obtained from least-squares refinement of the ordered part of the molecule range from 0.002 to 0.004 Å for bond lengths, and from 0.1 to 0.3° for bond angles.

The largest deformations on the C_{60} surface occur within the bridged pyracylene (= cyclopent[*fg*]acenaphthylene) subunits, as expected. With regard to an I_h-C_{60} fullerene, the bridgehead 6–6 bond lengths of the cyclohexene rings (1.596 Å), and the cyclopropane rings (1.591 to 1.617 Å) are increased by *ca.* 0.2 Å; the 6–5 bond lengths connected to the two kinds of bridgehead atoms (with mean values of 1.531 and 1.488 Å) are increased by *ca.* 0.08 and 0.04 Å, respectively.

The angular strain (*S*; based on the sum of the three bond angles at an atom) is significantly different for the two kinds of bridgehead atoms. For C(18) and C(36), the corresponding bond angles within the C_{60} skeleton (98.9 to 114.8°) give an average *S* value

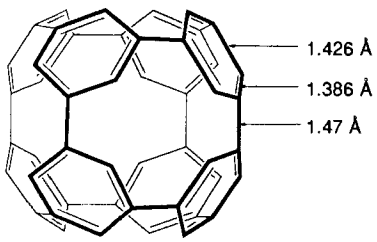

Fig. 4. *Schematic drawing of the cubic cyclophane substructure of the C_{60} skeleton not bridged to any of the functional groups*

of 327.6°; for C(1), C(22), C(23), and C(55) the corresponding bond angles (104.8 to 116.8°) give an average S value of 336.8°. (Note that if S is expressed in this way, it does not depend on the bond lengths, as does, for example, the distance of the atom from the plane of its three bonded neighbors.)

The five- and six-membered rings within the bridged pyracylene subunits show typical out-of-plane deformations towards an envelope or boat shape, respectively. The ring deformation produced by *Diels-Alder* addition is somewhat more pronounced than that produced by cyclopropanation. Within the five-membered rings, the bridgehead atoms in question deviate (from the corresponding four coplanar atoms) by *ca.* 0.31 and 0.17 Å, respectively; within the six-membered rings the two atoms out-of-plane deviate by *ca.* 0.14 and 0.07 Å, respectively.

With respect to the free C_{60} skeleton (with a mean diameter of *ca.* 7.07 Å [7]), the bridgehead atoms of the cyclohexene rings protrude out by *ca.* 0.24 Å, those of the cyclopropane rings by *ca.* 0.12 Å.

On the whole, the degree of deformation observed within the two kinds of pyracylene subunits in **1** is very similar to that found in corresponding C_{60} and C_{70} mono-adducts [8] [9].

Significant deformations also occur in the remaining part of the C_{60} skeleton. *Fig. 4* shows the subunit of eight unbridged six-membered rings, a network of benzene-like rings with approximate O_h symmetry. The average length of 6–6 and 6–5 bonds within these rings is 1.386 and 1.426 Å, respectively, and the mean inter-ring, biphenyl-type bond length is 1.471 Å. Compared with the free C_{60} skeleton, the bond-length alternation in these six-membered rings is reduced from *ca.* 0.06 to 0.04 Å (based on comparable X-ray values [7] [9b] [9d]), while the inter-ring distance is increased by *ca.* 0.02 Å. The same trend has been observed in the crystal structures of two analogous C_{60} hexakis-adducts [3] [4] and interpreted as an indication that the six-membered rings are becoming more benzene-like.

The anchor-tether-cyclohexene moiety (see *Fig. 2*) was designed *via* semi-empirical (PM3) calculations [10]. The ester group at the anchor (C(61), C(62), O(63), O(64), C(65)) is planar within 0.16 Å, the fragment C(65) to C(72) within 0.03 Å, and the benzene ring itself within 0.015 Å; moreover, the benzene ring is nearly parallel with a neighboring six-membered ring (C(8), C(9), C(10), C(24), C(25), C(26)) of the C_{60} skeleton, the mean inter-ring distance being 3.52 Å. The cyclohexene ring is boat-shaped; the angle between the mean planes C(74), C(75), C(76), C(77), and C(18), C(36), C(76), C(77) is 129.5°, a value close to those found in *Diels-Alder* mono-adducts of C_{60} and C_{70} [8]. The torsion

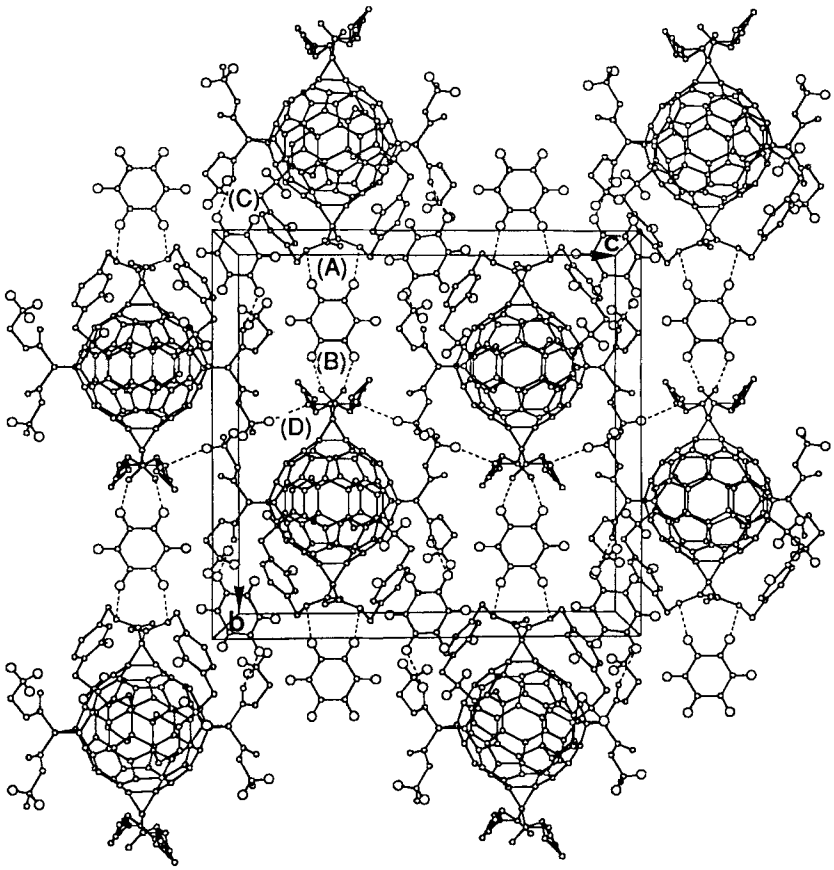

Fig. 5. *A layer of* **1** *and benzene molecules, parallel to the (1 0 0) plane, showing four different types of short C–H···O contacts (A)–(D).* Fullerene and benzene(1) molecules lie on twofold axes, benzene(2) on inversion centers.

angles of the fragments C(62)–O(64)–C(65)–C(66) and C(69)–C(72)–C(73)–C(74) are 84.1 and 65.3°, respectively.

The orientations of the EtO groups within the various diethyl-malonate residues differ considerably and are influenced possibly by short-range interactions (see below).

4. Crystal Packing. – 4.1. *Results.* The crystal packing of **1** (*Figs. 5* and *6*) is characterized by a three-dimensional network of (weak) C–H···O interactions between neighboring fullerenes, as well as between fullerene and benzene molecules. As mentioned, the fullerene and benzene(1) molecules lie on twofold axes, and benzene(2) on inversion centers. Each fullerene is involved in 14 short C–H···O contacts, *i.e.*, seven symmetry-related pairs (H-atoms of the disordered EtO groups are not considered in the present analysis, and only six types of contacts are shown in the packing drawings). Details of intermolecular contacts at 270, 230, and 180 K are summarized in *Table 2*. The estimation

Table 2. *Variation of the C–H···O Geometry of the Shortest Intermolecular Contacts as a Function of Temperature*[a])

	(A) C(102)–H(10C)···O(64)			(B) C(100)–H(10A)···O(91′)		
	H···O [Å]	C–H···O [°]	C···O [Å]	H···O [Å]	C–H···O [°]	C···O [Å]
270 K	2.46(2.47)	141(140)	3.377	2.51(2.59)	127(121)	3.280
230 K	2.45(2.46)	140(139)	3.362	2.49(2.44)	127(130)	3.255
180 K	2.40(2.38)	140(143)	3.313	2.50(2.39)	126(136)	3.263
	(C) C(103)–H(10D)···O(80)			(D) C(87)–H(87B)···O(92*′)		
	H···O [Å]	C–H···O [°]	C···O [Å]	H···O [Å]	C–H···O [°]	C···O [Å]
270 K	2.53(2.58)	125(121)	3.280	2.58(2.57)	155(156)	3.594
230 K	2.51(2.45)	125(130)	3.264	2.50(2.48)	156(159)	3.527
180 K	2.49(2.42)	126(131)	3.241	2.48(2.49)	156(153)	3.500
	(E) C(68)–H(68)···O(91)			(F) C(73)–H(73B)···O(80)		
	H···O [Å]	C–H···O [°]	C···O [Å]	H···O [Å]	C–H···O [°]	C···O [Å]
270 K	2.40(2.40)	134(134)	3.258	2.51(2.55)	148(143)	3.485
230 K	2.39(2.39)	133(133)	3.242	2.51(2.51)	148(149)	3.489
180 K	2.39(2.48)	132(125)	3.220	2.50(2.51)	150(149)	3.481
	(G) C(83)–H(83B)···O(81′)					
	H···O [Å]	C–H···O [°]	C···O [Å]			
270 K	2.41(2.40)	174(173)	3.491			
230 K	2.41(2.49)	177(154)	3.510			
180 K	2.46(2.50)	178(163)	3.555			

[a]) For each temperature, values based on calculated H-positions are given first, those based on least-squares refinement are given in parentheses. To account for the characteristic shortening, H-positions were moved along the corresponding C–H vectors to give (idealized) C–H distances of 1.09 Å. Contacts (A), (B), (C), and (E) contain C(arom.)–H proton donors, (D), (F), and (G) contain C(sp^3)–H proton donors. O(80) and O(91) are carbonyl O-atoms, O(64), O(81), and O(92*) are C(O)*O*R ester O-atoms.

of H-positions has been described in *Experimental*. Due to disorder, H···O distances and C–H···O angles at 180 K, are less reliable than those at the two higher temperatures, and results obtained at 100 K are omitted. From now on, values of H···O distances and C–H···O angles based on calculated (idealized) H-positions are given first (refinement A), those based on refined (idealized) H-positions (refinement B) are given in parentheses.

Fig. 5 shows a layer of **1** and solvent molecules parallel to the (1 0 0) plane of the monoclinic unit cell. In this plane, there are four types of C–H···O contacts denoted as (A), (B), (C), and (D). A striking feature is the chain built of alternating fullerene and benzene(1) molecules parallel to the *b*-axis; each benzene is in contact with opposite sides of two molecules of **1**, *i.e.*, with the C(O)*O*R ester O-atoms O(64) and O(64′) of the anchor-tether moiety (A), and with the carbonyl O-atoms O(91) and O(91′) of two EtO groups (B). The temperature dependence of the C(102)–H(10C)···O(64) geometry (A) between 270 and 180 K is similar for calculated and refined H-positions. The H···O distance in question decreases from 2.46(2.47) to 2.40(2.38) Å, the C···O distance

from 3.38 to 3.31 Å, and the C–H···O angle stays close to 140° (see *Table 2*). For C(100)–H(10A)···O(91′) contact (B), the corresponding H···O, C···O, and C–H···O values range from 2.51(2.59) to 2.49(2.39) Å, from 3.28 to 3.26 Å, and from 127(121) to 126(136)°, respectively, *i.e.*, values based on calculated and refined H-positions are appreciably different. It appears that the C–H···O geometries of contacts (A) and (B) are becoming more similar on cooling the crystal specimen to 180 K.

Benzene(2), sitting at the inversion center, makes short contacts with the carbonyl O-atoms O(80) and O(80′) of the ordered diethyl-malonate bridge at C(22)–C(23) (C); in the range 270 to 180 K, the H···O distance decreases from 2.53(2.58) to 2.49(2.42) Å, the C···O distance from 3.28 to 3.24 Å, and the corresponding C–H···O angle increases from 125(121) to 126(131)°, *i.e.*, the calculated H···O and C–H···O values stay almost constant, and the refined ones show a similar temperature behavior as in contact (B) (note that the carbonyl O-atoms O(80) and O(91) are involved in another short contact, discussed below).

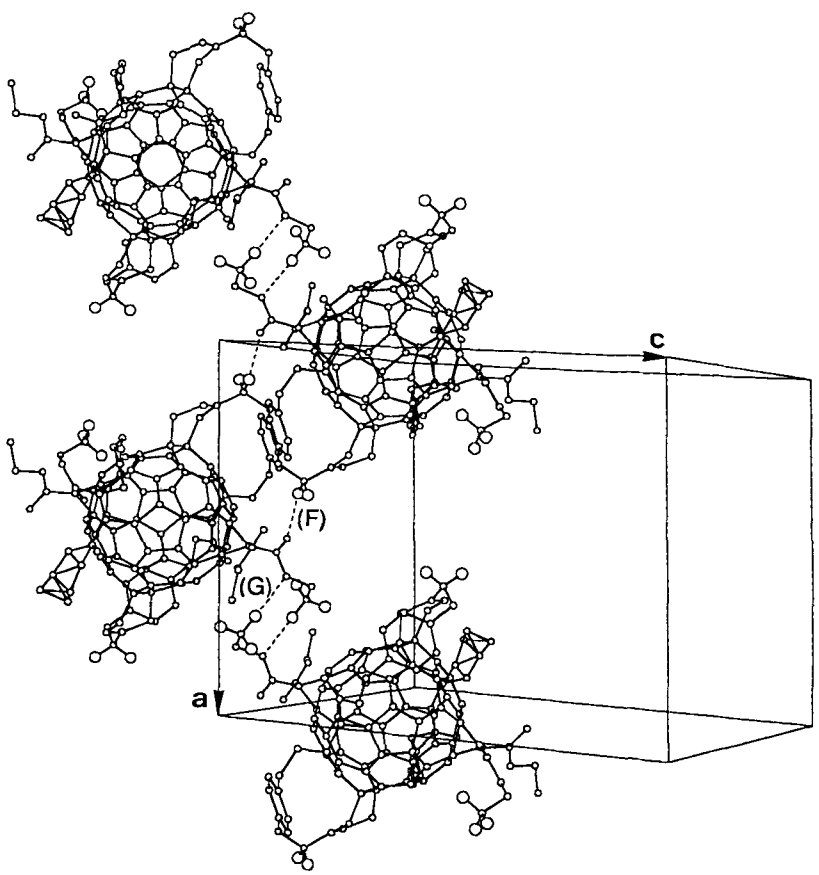

Fig. 6. *View of the crystal packing of* **1**, *showing two different types of short C–H···O contacts, (F) and (G), extending roughly along* a

Additional short intermolecular contacts occur roughly parallel to the *c*-axis between the disordered ester O-atom O(92*) and the C(87)H_2 group (D), and between the carbonyl O-atom O(91) and the (aromatic) proton donor C(68)H (E; not indicated). For the former contact, there is a pronounced decrease of H···O and C···O distances with decreasing temperature, namely from 2.58(2.57) to 2.48(2.49) Å, and from 3.59 to 3.50 Å, respectively, while the C–H···O angles stay close to 155(156)° throughout. For the latter contact, H···O distances range from 2.40(2.40) to 2.39(2.48) Å, C···O distances from 3.26 to 3.22 Å, and C–H···O angles from 134(134) to 132(125)°.

Fig. 6 shows two additional types of intermolecular C–H···O interactions, extending roughly along *a*. Contact (F), occurring between the carbonyl O-atom O(80) and the C(73)H_2 group of a neighboring tether moiety is almost invariant between 270 and 180 K, with average H···O, C···O, and C–H···O values of *ca.* 2.51(2.52) Å, 3.49 Å, and 149(147)°, respectively.

Contact (G), occurring between the ester O-atom O(81′) and the Me group C(83)H_3 of a neighboring molecule, and the corresponding symmetry-related contact form an eight-membered ring, as can be seen from *Figs. 6* and *7*. In contrast to the other examples described here, cooling of the crystal specimen leads to longer H···O and C···O distances, and based on refined H-positions to a reduction of the C(83)–H(83B)···O(81′) linearity. In the temperature range 270 to 180 K, the H···O distance increases from 2.41(2.40) to 2.46(2.50) Å, the C···O distance from 3.49 to 3.55 Å; the corresponding C–H···O angle (based on refined H-positions) shows an irregular behavior, *i.e.*, values obtained at 270, 230, and 180 K are 174(173), 177(154), and 178(163)°, respectively.

4.2. *Discussion.* The derived H···O and C–H···O values are undoubtedly contaminated by systematic and random errors. Nevertheless, the results, based on three different temperatures and two different crystal specimens, contain some characteristic features.

Firstly, the intermolecular geometry of contacts (A), (B), (C), and (E), containing C(arom.)–H proton donors is quite different from the geometry of contacts (D), (F), and (G), containing C(sp^3)–H proton donors. The C···O distances derived in the first group (3.22 to 3.38 Å) are much shorter than those derived in the second group (3.49 to 3.60 Å).

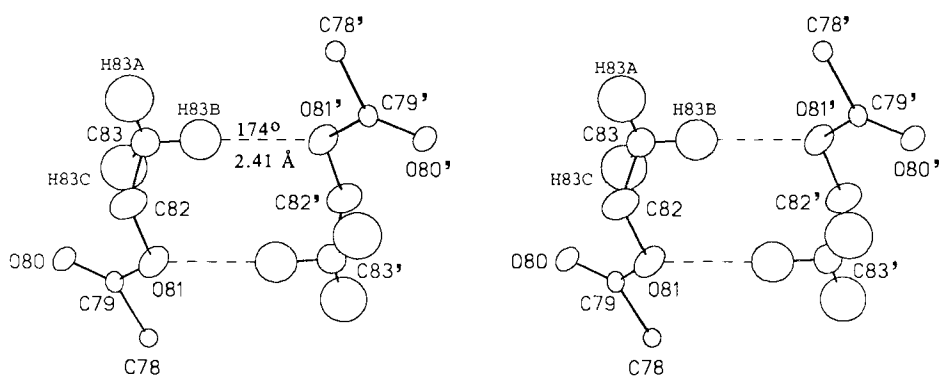

Fig. 7. *Stereoview of the eight-membered ring, formed by two symmetry-related short C–H···O contacts (G).* Vibrational ellipsoids obtained at 270 K are shown at the 20% probability level.

The H···O distances derived at 230 and 180 K show a similar trend. In fact, neglecting contact (E), the H···O distances (based on refined H-positions) obtained at 180 K for the two types of contacts are close to 2.4 and 2.5 Å, respectively. The C–H···O angle is also different, and clearly more linear in the second group. Significant differences of the C–H···O geometry, due to the two kinds of O-atoms, are not apparent on this level of accuracy. On the other hand, *Table 2* shows that both carbonyl O-atoms are involved in two short contacts, while the C(O)*O*R ester O-atoms are involved in only one. To what extent the geometrical differences are characteristic, and to what extent they are imposed by the overall arrangement of the two types of molecules is not obvious.

Secondly, the present analysis provides information about the nature of short-range interaction. For example, the continuous decrease of intermolecular distances of contacts (A), (B), (C), and (D) suggests that these interactions are attractive in nature, while the observed H···O increase of contact (E) between 230 and 180 K may be an indication of increasing short-range repulsion (or result from disorder). What is the nature of contacts (F) and (G), occurring roughly along *a*? For C(73)–H(73B)···O(80) contact (F), intermolecular distances and angles are nearly constant within the investigated temperature range, and, hence, a classification is not unequivocal in this case. The C(83)–H(83B)···O(81′) contact (G) within the eight-membered ring seems to be repulsive, at least below 270 K, since cooling of the crystal specimen leads to longer H···O and C···O distances, and (based on refined H-positions) to reduction of the C–H···O linearity.

This apparent intermolecular expansion within the eight-membered ring is not completely understood. In principle, it could result from an ordering process of the two Me groups or from a reduction of anharmonic internal rotational motion of the ester groups involved, or from a combination of both effects. The minimal changes in the torsion angles (between 270 and 180 K) of the fragments C(79)–O(81)–C(82)–C(83) (−83° to −80°), and O(81)–C(82)–C(83)–H(83B) (−60° to −59°) suggest that the latter effect is small (note that such small changes of the torsion angles could also be produced by intermolecular repulsion along the C(83)–H(83B)···O(81′) contact).

There are several indications that the observed intermolecular expansion is associated with an ordering process of the Me groups involved. Firstly, it is indeed surprising that the apparently strongest intermolecular interaction occurs between a Me H-atom and an ester O-atom (*i.e.*, between a poor proton donor and a poor proton acceptor; *Vedani*, personal communication). Secondly, lowering of the crystal temperature must reduce the flipping-rate of these Me groups. Thirdly, the anomalous thermal expansion of *a* below *ca.* 200 K, the increasing disorder at low temperature (which manifests itself by artificially anisotropic displacement parameters and high $R(F)$ values), and the destruction of the crystal specimens (below *ca.* 200 K, see *Sect. 2.3*) are all compatible with increasing intermolecular (repulsive) interactions with decreasing temperature. Fourthly, preliminary electron-density analyses suggest that the vibrational motion of H(83B) roughly perpendicular to the mean plane of the eight-membered ring (shown in *Fig. 7*) is quite pronounced at 270 and 230 K, and that the Me group is slightly disordered at 180 K. The observed anisotropy of H(83B) could be interpreted in terms of alternate positions above and below the mean plane. In this case, the O···H distance of 2.4 Å, obtained at 270 K would be too short, since the H-position would represent an average. In principle, this model could be tested by following the librational motion of this Me group as a function

of temperature, but with the present X-ray data, such an approach would give meaningless results.

Whatever the exact ordering process may be, its net effect must lead to an increase of the electron density along the C(83)–H(83B)···O(81′) axis, and, in turn, to an increase of the short-range repulsion, which is essentially due to overlap of the electron-density distribution of proton-donor and proton-acceptor atoms [11].

In the last 20 years, C–H···O H-bonding has been established in numerous crystal structures, even for C(sp^3)–H···O contacts (see, *e.g.*, *Taylor* and *Kennard* [12]; *Seiler et al.* [13]; *Desiraju* [14]; *Bernstein et al.* [15]). Nevertheless, reliable characterization of such weak interactions is not a trivial matter, as is evident from the present analysis. In fact, in a routine analysis, the shortest, nearly linear C(sp^3)–H···O contact in **1** (based on calculated intermolecular distances and angles) could easily be classified as attractive. Also, it is unlikely that this example represents a special case, since, when a molecule is involved in various stronger and weaker short-range interactions, not all of them must necessarily contribute to the stabilization of the crystal packing.

In retrospect, the crystal-mounting procedure (covering the crystal specimen with epoxy resin) was not optimal, since the solvent is obviously bound in the crystal. However, without this precaution (and the resulting problems), we would have overlooked an interesting aspect of the crystal packing of **1**.

We are grateful to Prof. *Jack D. Dunitz* for his constructive comments on the manuscript.

REFERENCES

[1] L. Isaacs, R. F. Haldimann, F. Diederich, *Angew. Chem.* **1994,** *106,* 2434; *ibid. Int. Ed.* **1994,** *33,* 2339.
[2] L. Isaacs, P. Seiler, F. Diederich, *Angew. Chem.* **1995,** *107,* 1636; *ibid. Int. Ed.* **1995,** *34,* 1466.
[3] P. J. Fagan, J. C. Calabrese, B. Malone, *J. Am. Chem. Soc.* **1991,** *113,* 9408.
[4] I. Lamparth, C. Maichle-Mössmer, A. Hirsch, *Angew. Chem.* **1995,** *107,* 1755; *ibid. Int. Ed.* **1995,** *34,* 1607.
[5] J. D. Dunitz, P. Seiler, *Acta Crystallogr., Sect. B* **1973,** *29,* 589.
[6] R. Taylor, *J. Chem. Soc., Perkin Trans. 2* **1993,** 813.
[7] H. B. Bürgi, E. Blanc, D. Schwarzenbach, S. Liu, Y.-j. Lu, M. M. Kappes, J. A. Ibers, *Angew. Chem.* **1992,** *104,* 667; *ibid. Int. Ed.* **1992,** *31,* 640.
[8] a) F. Diederich, U. Jonas, V. Gramlich, A. Herrmann, H. Ringsdorf, C. Thilgen, *Helv. Chim. Acta* **1993,** *76,* 2445; b) Y. Rubin, S. Khan, D. I. Freedberg, C. Yeretzian, *J. Am. Chem. Soc.* **1993,** *115,* 344; c) P. Belik, A. Gügel, A. Kraus, J. Spickermann, V. Enkelmann, G. Frank, K. Müllen, *Adv. Mater.* **1993,** *5,* 854; d) P. Seiler, A. Herrmann, F. Diederich, *Helv. Chim. Acta* **1995,** *78,* 344.
[9] a) J. Osterodt, M. Nieger, F. Vögtle, *J. Chem. Soc., Chem. Commun.* **1994,** 1607; b) H. L. Anderson, C. Boudon, F. Diederich, J.-P. Gisselbrecht, M. Gross, P. Seiler, *Angew. Chem.* **1994,** *106,* 1691; *ibid. Int. Ed.* **1994,** *33,* 1628; c) E. F. Paulus, C. Bingel, *Acta Crystallogr., Sect. C* **1995,** *51,* 143; d) P. Timmerman, H. L. Anderson, R. Faust, J.-F. Nierengarten, T. Habicher, P. Seiler, F. Diederich, *Tetrahedron* **1996,** *52,* 4925.
[10] L. Isaacs, ETH Dissertation 11247, Zürich 1995.
[11] H. Umeyama, K. Morokuma, *J. Am. Chem. Soc.* **1977,** *99,* 1316.
[12] R. Taylor, O. Kennard, *J. Am. Chem. Soc.* **1982,** *104,* 5063.
[13] a) P. Seiler, G. R. Weisman, E. D. Glendening, F. Weinhold, V. B. Johnson, J. D. Dunitz, *Angew. Chem.* **1987,** *99,* 1216; *ibid. Int. Ed.* **1987,** *26,* 1175; b) P. Seiler, J. D. Dunitz, *Helv. Chim. Acta* **1989,** *72,* 1125.
[14] G. R. Desiraju, *Acc. Chem. Res.* **1991,** *24,* 290.
[15] J. Bernstein, M. C. Etter, L. Leiserowitz, 'The role of hydrogen bonding in molecular assemblies', in 'Structure Correlation Vol. 2', Eds. H.-B. Bürgi and J. D. Dunitz, VCH Verlagsgesellschaft, Weinheim, 1994, pp. 431–507, and ref. cit. therein.